Large-scale photonic crystals with inserted defects and their optical properties*

Li Chao-Rong(李超荣)†, Li Juan(李 娟), Yang Hu(杨 虎), Zhao Yong-Qiang(赵永强), Wu Yan(吴 艳), Dong Wen-Jun(董文钧), and Chen Ben-Yong(陈本永)

Department of Physics and Key Laboratory of ATMMT Ministry of Education, Zhejiang Sci-Tech University, Hangzhou 310018, *China*

(Received 8 January 2014; revised manuscript received 27 February 2014; published online 20 June 2014)

Deliberately introducing defects into photonic crystals is an important way to functionalize the photonic crystals. We prepare a special large-scale three-dimensional (3D) photonic crystal (PC) with designed defects by an easy and low-cost method. The defect layer consists of photoresist strips or air-core strips. Field emission scanning electron microscopy (FESEM) shows that the 3D PC is of good quality and the defect layer is uniform. Different defect states shown in the ultraviolet-visible spectra are induced by the photoresist strip layer and air-core strip layer. The special large-scale 3D PC can be tested for integrated optical circuits, and the defects can act as optical waveguides.

Keywords: photonic crystal, designed defects, photolithography, defect state

PACS: 81.16.Dn, 61.72.Nn, 81.16.Rf, 81.16.–c **DOI:** 10.1088/1674-1056/23/8/088114

1. Introduction

Photonic crystals (PCs) are periodic optical nanostructures leading to photonic band gaps or stop bands with a depleted photonic density of states, that is, the structures can suppress or guide the propagation of electromagnetic radiation in a specific wavelength range. PCs have attracted increasing attention since their advent in 1987[1,2] because of the potential applications in photonics, such as optical chips, sensors, and laser microcavities.[3] Great efforts have contributed to the minimization of the presence of intrinsic defects like cracks, dislocations or stacking faults to obtain large-scale PCs with excellent structural and optical qualities.[4,5]

On the contrary, some optical applications of PCs, such as low-loss waveguides, resonant cavities, zero-threshold microlasers, light-emitting diodes, optical switches, optical fibers, all-optical transistors, and tunable filters require well-designed defects in the interior of the PCs.[6,7] Therefore, we can harness the properties of PCs by controlling the introduction of defects into the crystal leading to defect states within the photonic gaps.[8] Defect engineering for self-assembled PCs has garnered ever-increasing interest from scientific researchers.[9,10]

To date, numerous techniques have been successfully developed for constructing deterministic defects, including multi-photon polymerization,[11,12] nanoimprinting lithography,[13] laser writing,[14] photolithography,[15,16] and direct electron-beam writing techniques.[17]The Langmuir–Blodgett technique, the vertical deposition method, and spin-coating have been used to embed a monolayer of spheres of different sizes[18,19] or different dielectric strengths into PCs.[20] Planar defects also have been fabricated by chemical vapor deposition (CVD),[21,22] inverting a silica defect slab between two PCs films. Scientists have also introduced two-dimensional (2D) luminescent organic defect layers within PCs via a versatile room-temperature remote plasma deposition process.[23] While these methods are precise and have design flexibility, they are often limited to small areas and cannot possess the optical properties influenced by the defects.

In this paper, we demonstrate the preparation of a large-scale 3D PC possessing designed defects by a combination of the evaporation-induced assembly method and photolithography. Photolithography supplies an effective means to prepare defects assembled by micron level and uniform photoresist or air-core strips. Hence, the PC displays special functions at ultraviolet-visible (UV–vis) wavelengths, which opens up possibilities for controlling and modulating the flow of light.

2. Experimental section

2.1. Synthesis of the particles

The monodisperse SiO_2 nanoparticles (384 nm in diameter, standard deviation approximately 3.58%) were prepared by the Stober method.[24] –COOH functional groups can replace –OH functional groups conjugated to the surface of synthesized SiO_2 nanoparticles through a silane-coupling reaction. 0.1-g succinic anhydride was dissolved in 30-ml N, N-dimethylformamide (DMF), and 1-ml KH550 was added to the suspension with vigorous stirring. After the 3-hour reaction at 75 °C, 0.1-g SiO_2 nanoparticles were added into the KH550–COOH solution, stirring for 5 h. The whole reaction

*Project supported by the National Natural Science Foundation of China (Grant Nos. 91122022 and 51172209) and the Program for Changjiang Scholars and Innovative Research Team (PCSIRT) in University, China (Grant No. IRT13097).

†Corresponding author. E-mail: crli@zstu.edu.cn

© 2014 Chinese Physical Society and IOP Publishing Ltd

was under the protection of N_2 and in an oil bath at 75 °C. Finally, the products were washed three times with water and absolute ethanol, sequentially. The SiO_2 nanoparticles modified with –COOH were dried in a vacuum oven at 60 °C and kept there until they became powder. The –COOH functional groups supply stronger Van der Waals forces than the –OH functional groups to prompt SiO_2 nanoparticles to form an ordered structure during assembly.

2.2. Fabrication of PCs with designed defects

The multi-step method to fabricate the 3D PCs with designed defects is shown in Fig. 1. Firstly, the modified SiO_2 nanoparticles were assembled on the prepared hydrophilic substrate (the quartz glass slides were 1.25 cm×5 cm scale pieces and underwent hydrophilic processing in piranha solution) via an evaporation-induced assembly method to form an original PC. That is, the substrate was dipped in the 10-ml beaker with 6-mL 0.08-wt% modified SiO_2 nanoparticle suspension. The system was placed in a 60-°C vacuum oven for 48 h to evaporate the deionized water.

Secondly, photoresist was spin-coated on the surface of the original PC at a speed of 2500 r/min for 50 s. UV contact photolithography was applied to pattern strips with an exposure time of 45 s. After developing for 20 s, photoresist strips were formed.

Thirdly, the evaporation-induced assembly method was used again to grow another PC on the surface of the original PC with photoresist strips.

Finally, the PC embedded photoresist strips were soaked in acetone for 8 h to remove the photoresist. Therefore, specially designed structures inserted into photoresist strips or air-core strips were prepared.

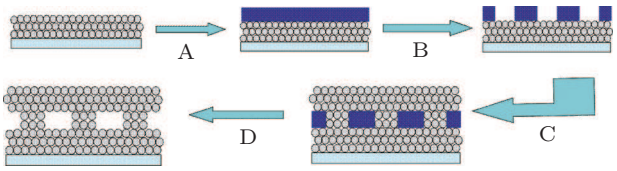


Fig. 1. (color online) A diagram of the method of fabricating defects in a 3D PC. (A) Photoresist is spin-coated on the surface of an original PC. (B) The photoresist layer is patterned to become strips through photolithgraphy. (C) Another PC is grown to complete the insertion of photoresist strips in a 3D PC. (D) The inserted photoresist strips are removed by soaking samples in acetone for 8 h. The 3D PC inserted into the air-core strips is prepared.

2.3. Characterization

The spectra of SiO_2 nanoparticles and modified SiO_2 nanoparticles were measured by Fourier transform infrared spectroscopy (FTIR) (Nicolet Avatar 370) to characterize the functional groups on the surfaces of the nanoparticles. FTIR spectra of the samples were measured using KBr tablets (1% w/w of product in KBr). The morphologies of the designed structures were observed by a field emission scanning electron microscope (FESEM) (Hitachi S-4800). The optical properties of the PCs were investigated by a UV–vis spectrophotometer (Hitachi U-3900). The films prepared at each step were measured by using the mode of UV–vis transmission, and the contribution from quartz glass serving as a substrate was deducted.

3. Results and discussion

3.1. Characterization of surface functionalization

As is well known, the electrostatic force between SiO_2 nanoparticles plays an important role in self-assembly. The SiO_2 nanoparticles modified with –COOH provide a stronger electrostatic force than the normal SiO_2 nanoparticles whose surfaces were coated by –OH. Figure 2 shows the FTIR spectra of SiO_2–OH nanoparticles and SiO_2-COOH nanoparticles. The peaks at about 800 cm^{-1} and 1100 cm^{-1} are the symmetric stretching vibration peaks at the horizontal and vertical planes of the bonds of Si–O–Si respectively. The peak at 3414 cm^{-1} is the stretching vibration of the bond of O–H. The FTIR spectrum of SiO_2–COOH nanoparticles confirms the successful functionalization of SiO_2 nanoparticles by the presence of a carbonyl group (–CO–, $\nu_{C=O} \approx 1560\ cm^{-1}$) and hydroxyl group (–OH, $\nu_{O-H} \approx 3448\ cm^{-1}$).[25] Influenced by –CO–, the peak of –OH has a red shift relative to the normal –OH.

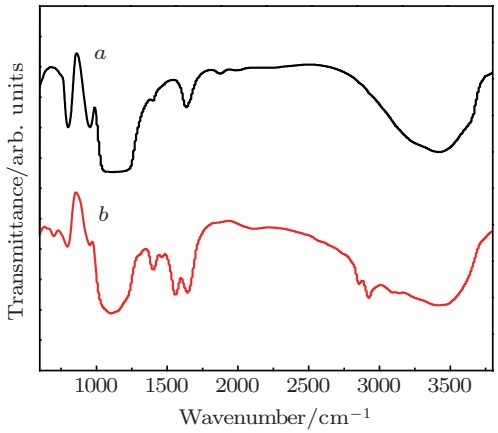


Fig. 2. (color online) FTIR spectra of dried SiO_2 nanoparticles (curve *a*) and –COOH-modified SiO_2 nanoparticles (curve *b*).

3.2. Structure and morphology

The FESEM images shown in Fig. 3 depict a 3D PC with embedded designed defects obtained in each step. It is seen from Figs. 3(a) and 3(b) that a PC possesses a face-centered cubic (fcc) close-packed structure with the (111) plane parallel to the substrate surface, and the inset FFT images of panels (a) and (b) also convincingly confirm that.

Photoresist strips on the surface of an original PC are observed in Figs. 3(c) and 3(d). They are not cuboid strictly because of the diffraction effects on the edge of the photomask

and photoresist in the photoetching process. The thickness values of the strips can be tuned by changing the spin-coating speed and time with their corresponding exposure and development time. Some photoresist infiltrated into the voids of nanoparticles below the strips is not removed completely after developing, which can be seen from the inset of Fig. 3(d).

After growing another PC, photoresist strips are embedded in a PC successfully as shown in Figs. 3(e) and 3(f). The inset FFT image of Fig. 3(e) shows that the periodicity of regrown PC is not so perfect as the original PC film because of the roughness on the PC surface. The inset of Fig. 3(f) also shows that the SiO_2 nanoparticles grown on the photoresist are assembled better than on the original PC.

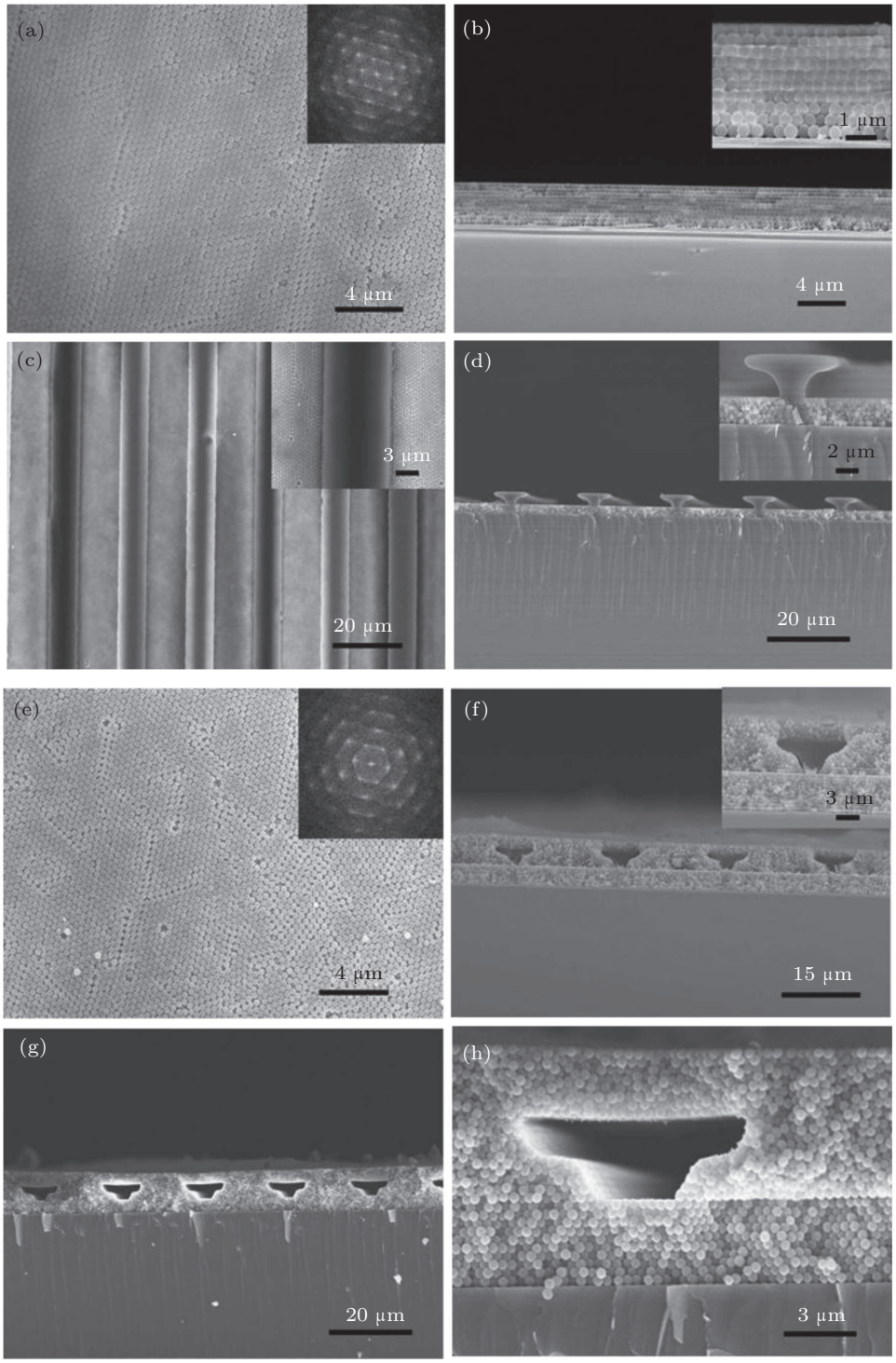


Fig. 3. FESEM images of (a) plane view and (b) cross section of an original PC, (c) plane view and (d) cross section of the PC with photoresist strips, (e) plane view and (f) cross section of the 3D PC with embedded photoresist strips, cross sections of a 3D PC with embedded air-core strips at low (g) and high (h) magnifications. The insets of panels (a) and (e) show the fast Fourier transform (FFT) images. The insets of panels (b), (c), (d), and (f) show the magnified FESEM images, correspondingly.

The images of Figs. 3(g) and 3(h) with different magnifications clearly prove that a 3D PC inserted into the air-core strips is prepared successfully. The close-packed hexagonal phase does not change in the process of soaking in acetone for 8 h. The image in Fig. 3(h) also shows that the photoresists infiltrated into the original PC voids are removed completely. The images in Figs. 3(f) and 3(g) reveal that the specially prepared structures are sized at the micron level.

3.3. Optical properties

The inserted photoresist strip layer and air-core strip layer introduce localized defect states into the band gaps, which are characterized by UV–vis. The squares curve in Fig. 4 presents that the central wavelength of the photonic band gap (PBG) in a PC film is 830 nm.

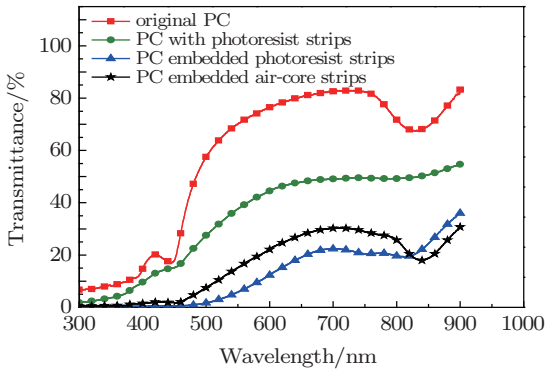


Fig. 4. (color online) UV–vis transmission spectra of an original PC (squares), the PC with photoresist strips (circles), the PC with embedded photoresist strips (triangles), and the PC with embedded air-core strips (stars).

The PBG position in PC can be estimated by Bragg's law of diffraction, which is obtained by combining the law of reflection with Snell's law and considering the conditions for interference,[26] as follows:

$$m\lambda = 2d_{(hkl)}\sqrt{(n_{\text{avg}}^2 - \sin^2\alpha)}, \tag{1}$$

where m is the order of reflection for which interference occurs; λ is the light wavelength; $d_{(hkl)}$ is the interplanar spacing of the (hkl) lattice plane, and $d_{(hkl)} = \sqrt{2}D/\sqrt{h^2+k^2+l^2}$ with D being the diameter of the SiO_2 nanoparticles; n_{avg} is the average refractive index of PC, and $n_{\text{avg}} = f_{\text{sphere}} \times n_{\text{sphere}} + (1 - f_{\text{sphere}}) \times n_{\text{air}}$, in which f is the volume fraction of spheres and generally $f = 74\%$ in an fcc structure, and n_{sphere} and $n_{\text{interspace}}$ are the refractive indices of the material of the sphere and interspace, respectively; α is the incident angle, which equals 0°. According to Eq. (1), the PBG position of a PC film is 833 nm and this is consistent with the experimental result of 830 nm.

The photoresist strips on the surface of the PC lead to the expected disappearance of the Bragg peak because the periodicity is interrupted. The photoresist strips form a 2D periodical structure with vertical incident light, which also shows no peak. After the photoresist strip layer and the air-core strip layer are inserted, the Bragg peaks reappear and show an inter gap defect state.

Bragg diffraction is caused by constructive interference which happens when an incident ray reflects from different lattice planes. The inserted defect layer will cause a phase shift, due to the variation of the average refractive index. There, the inserted layer will then disturb the interference condition. Consequently, the Bragg diffraction will then be changed.

Equation (1) is used widely in the literature for calculating PBGs of PCs. By a more rigorous treatment through using dynamical diffraction theory, the peak position λ is changed into λ_{D}[26] as given as

$$\lambda_{\text{D}} = \lambda\left(1 + \frac{\psi}{2}\right), \tag{2}$$

where ψ can be estimated by the following equation:

$$\psi = 3\phi\frac{r^2-1}{r^2+2}, \tag{3}$$

where, ϕ is the solid fraction in the material, r is the ratio of the refractive index of the walls to that of the voids (i.e., $r = n_{\text{walls}}/n_{\text{voids}}$).

Here, the inserted photoresist strips or air-core strips behave as a new phase different from assembled PC. The values of r equal $n_{\text{avg}}/n_{\text{photoresist}}$ and $n_{\text{avg}}/n_{\text{air}}$, ($n_{\text{avg}} = 1.33$, $n_{\text{photoresist}} = 1.5$, $n_{\text{air}} = 1$), respectively. According to Eqs. (2) and (3), PBG positions of PCs with embedded photoresist strips and air-core strips respectively have a little blue shift and red shift, which correspond to the triangle and star lines shown in Fig. 4.

4. Conclusions

In this paper, we describe the fabrication of a large-scale PC with embedded designed defects consisting of uniform photoresist strips or air-core strips, using an effective method. The thickness of the defect layer can be adjusted by changing the photoresist spin-coating speed and time. The different gap defect states induced by the designed defects are confirmed by transmission spectra of the samples and analyzed by Bragg's law of diffraction. The air-core strips open up possibilities for inserting defects composed of many kinds of components in a chemically and thermally robust PC, such as a range of high-refractive-index materials. The introduced PCs have applications in large-scale optical components, such as laser sources, chemically tunable filters, etc.

References

[1] Yablonovitch E 1987 *Phys. Rev. Lett.* **58** 2059
[2] John S 1987 *Phys. Rev. Lett.* **58** 2486
[3] Jiang H T, Li Y H, Li H Q, Zhu R L, Zhang Y W and Chen H 2003 *Physics* **32** 799 (in Chinese)

[4] Zhang Q, Meng Q B, Cheng B Y and Zhang D Z 2004 *Acta Phys. Sin.* **53** 58 (in Chinese)
[5] Chabanov A A, Jun Y and Norris D J 2004 *Appl. Phys. Lett.* **84** 3573
[6] Joannopoulos J D, Johnson S G, Winn J N and Meade R D 2008 *Photonic Crystals: Molding the Flow of Light*, 2nd edn. (Princeton: Princeton University Press) p. 137
[7] Zhen W H, Ren G, Xing M X, Du X Y, Wang K, Zhang Y J and Chen L H 2007 *Physics* **36** 619 (in Chinese)
[8] Yablonovitch E, Gmitter T J, Meade R D, Rappe A M, Brommer K D and Joannopoulos J D 1991 *Phys. Rev. Lett.* **67** 3380
[9] Liu Y Z and Li Z Y 2008 *Physics* **37** 658 (in Chinese)
[10] Wang L, Yan Q and Zhao X S 2006 *Langmuir* **22** 3481
[11] Jun Y, Leatherdale C A and Norris D J 2005 *Adv. Mater.* **17** 1908
[12] Lee W, Pruzinsky S A and Braun P V 2002 *Adv. Mater.* **14** 271
[13] Yan Q, Chen A, Chua S J and Zhao X S 2005 *Adv. Mater.* **17** 2849
[14] Tétreault N, Míguez H, Yang S M, Kitaev V and Ozin G A 2003 *Adv. Mater.* **15** 1167
[15] Yan Q, Zhou Z, Zhao X S and Chua S J 2005 *Adv. Mater.* **17** 1917
[16] Vekris E, Kitaev V, von Freymann G, Perovic D D, Aitchison J S and Ozin G A 2005 *Adv. Mater.* **17** 1269
[17] Ferrand P, Seekamp J, Egen M, Zentel R, Romanov S G and Sotomayor Torres C M 2004 *Microelectronic Engineering* **73** 362
[18] Wang A J, Chen S L, Dong P, Cai X G, Zhou Q, Yuan G M, Hu C T and Zhang D Z 2009 *Chin. Phys. Lett.* **26** 024210
[19] Zhao Y, Wostyn K, de Schaetzen G, Clays K, Hellemans L, Persoons A, Szekeres M and Schoonheydt R A 2003 *Appl. Phys. Lett.* **82** 3764
[20] Fleischhaker F, Arsenault A C, Schmidtke J, Zentel R and Ozin G A 2006 *Chem. Mater.* **18** 5640
[21] Tétreault N, Mihi A, Míguez H, Rodríguez I, Ozin G A, Meseguer F and Kitaev V 2004 *Adv. Mater.* **16** 346
[22] Palacios-Lidón E, Galisteo-López J F, Juárez B H and López C 2004 *Adv. Mater.* **16** 341
[23] Fleischhaker F, Arsenault A C, Kitaev V, Peiris F C, von Freymann G, Manners I, Zentel R and Ozin G A 2005 *J. Am. Chem. Soc.* **127** 9318
[24] Stober W, Fink A and Bohn E. J 1986 *Colloid Interface Sci.* **26** 62
[25] Liu K and Jiang L 2011 *Nano Today* **6** 155
[26] Aguirre C I, Reguera E and Stein A 2010 *Adv. Funct. Mater.* **20** 2565